JOURNAL OF Materials CHEMISTRY

Microspheres of the gas sensor material $Cr_{2-x}Ti_xO_3$ prepared by the sol–emulsion–gel route

Gilles Chabanis, Ivan P. Parkin* and David E. Williams

Department of Chemistry, University College London, 20 Gordon Street, London, UK WC1H OAJ. E-mail: i.p.parkin@ucl.ac.uk

Received 18th December 2000, Accepted 15th March 2001
First published as an Advance Article on the web 4th April 2001

Chromium titanium oxide (CTO) $Cr_{2-x}Ti_xO_3$ ($x=0.05$ to 0.4) is the first gas-sensitive resistor material successfully to be commercialised since tin dioxide in the 1960s. Microspheres were synthesised by the sol–emulsion–gel method and characterised by X-ray diffraction, scanning electron microscopy (SEM/EDAX) and X-ray photoelectron spectroscopy (XPS). Three differently sized microspheres of size 10, 2 and 0.7 μm were synthesised. The microspheres showed minimal variation in size and good compositional homogeneity. The CTO powders fired at 1000 °C crystallised as single phases for $Cr_{1.95}Ti_{0.05}O_3$, $Cr_{1.9}Ti_{0.1}O_3$ and $Cr_{1.8}Ti_{0.2}O_3$. For $x>0.2$ the formation of a secondary $CrTiO_3$ phase was noted. EDAX and XPS measurements revealed the absence of impurities and a surface segregation of the Ti atoms.

Titanium substituted chromium oxides (CTO), $Cr_{2-x}Ti_xO_{3+y}$, have been developed successfully as gas sensitive resistors at elevated temperatures for the detection of combustible and toxic gases.[1–5] The technique generally used for the preparation of titanium substituted chromium oxides consists of a solid state reaction between chromium and titanium oxide.[1,6] The Cr_2O_3 and TiO_2 powders are mixed, milled and calcined to achieve the solid state reaction. The potential disadvantages of this method are poor chemical homogeneity, introduction of chemical impurities during the milling stage and poor control of the microstructure during sintering. Sintering, impurities and non-homogeneity are known to have an influence on the gas sensor response. Variations in microstructure have a very significant effect on the behaviour. The development of powders with tailored properties is of major importance for the improvement of the selectivity, sensitivity and reproducibility of gas sensors.

The sol–gel method has proved to be an excellent means to control particle size, shape and the degree of impurity in materials synthesis.[7–15] However much of the work has focused on the synthesis of ceramics for plasma spray coating[7–15] or of tin dioxide powders for gas sensor applications[16–20] and no work has been reported on the preparation of titanium substituted chromium oxides by the sol–gel technique.

This paper reports the synthesis and characterisation of titanium substituted chromium oxide spherical particles of controlled particle size using the sol–emulsion–gel route. Some preliminary data on the gas sensing properties of the $Cr_{2-x}Ti_xO_3$ materials are also reported.

Experimental

Chromium nitrate nonahydrate 99% ($Cr(NO_3)_3{\cdot}9H_2O$), titanium(IV) isopropoxide 98% ($Ti[OCH(CH_3)_2]_4$), triethylamine 99% ($[C_2H_5]_3N$) and sorbitan monooleate (span 80) were obtained from Aldrich Chemical Co. and used as supplied.

Compounds of nominal composition $Cr_{2-x}Ti_xO_{3+y}$ ($x=0.05$, 0.1, 0.2, 0.4) were prepared by the sol–emulsion–gel technique. The preparative process involves two steps: (i) preparation of compatible chromia and titania sols that can be mixed in the required proportion, and (ii) formation of gel microspheres by producing an emulsion of sol droplets and their subsequent neutralisation with a base.

Preparation of the chromia sol

The chromia sol (Cr_2O_3) was prepared from de-ionisation of aqueous chromium nitrate (1 M) by a triethylamine (TEA) solution in 1,1,1-trichloroethane.[7]

A part of the nitrate was extracted by the addition of the TEA solution. Two layers of liquid were produced in this step, *i.e.* an aqueous phase with Cr^{3+} and a heavier organic phase with the extracted nitrate. The aqueous chromium nitrate enriched in OH^- (see equation (1)) led to the formation of the sol.

$$p\mathrm{Cr(NO_3)_3}+q(\mathrm{H_2O})+m\mathrm{Et_3N}\rightleftharpoons \mathrm{Cr}_p(\mathrm{NO_3})_{3p-m}(\mathrm{OH})_m+m\mathrm{Et_3N(HNO_3)}+(q-m)\mathrm{H_2O} \quad (1)$$

Chromium nitrate nonahydrate (160 g, 0.4 mol) was diluted in 400 ml of distilled water. Then, the aqueous chromium nitrate (1 M) was stirred for 5 minutes with 29.7 ml of TEA diluted in 1,1,1-trichloroethane to give an approximately 1 M solution. The phases were separated and the aqueous phase was extracted with a second 29.7 ml of TEA (1 M). This procedure was repeated a total of three times, each extraction producing an aqueous phase with a lower NO_3^-/Cr^{3+} ratio. The final NO_3^-/Cr^{3+} molar ratio was kept to 1.4 for all the chromia sols prepared. Further extraction beyond this limit led to relatively quick formation of the gel. The final concentration of the chromia sol was 0.87 mol l^{-1}.

Preparation of the titania sol

The titania sol (TiO_2) was prepared *via* the hydrolysis and condensation of titanium isopropoxide under a large excess of water acidified with nitric acid.[21–23] Nitric acid was used as both a hydrolysis catalyst and a peptizing agent.

A typical titania sol preparation consisted of mixing 6.25 ml of HNO_3 (10 M) with 500 ml of distilled water (22.7 mol) in a glass bottle maintained at 50 °C in a temperature-controlled bath. The pH, measured with a pH meter calibrated using a standard solution (pH = 7), was 1.2. The mixture was stirred at high speed (8000 rpm) and 37.2 ml of titanium isopropoxide (0.126 mol) was added dropwise over 15 minutes. The hydrolysis and condensation reactions started immediately as indicated by the rapid increase in turbidity. After a period of 2 hours, a clear light-blue solution of concentration of 0.25 mol l^{-1} TiO_2 was formed.

DOI: 10.1039/b010049h

Table 1 Preparation characteristics of the emulsion for the three procedures: Fabrication of four powders ($x=0.05$, 0.1, 0.2 and 0.4) with procedure A, three powders ($x=0.05$, 0.1 and 0.4) with procedure B and two compounds ($x=0.05$ and 0.1) with procedure C

Procedure	Hexane/sol (vol ratio)	Surfactant (vol%)	Stirring rate (rpm)
A	3	1.5	2000
B	3	1.5	8000
C	3	1.5	20500

Preparation of the chromia–titania sol and formation of the gel

The chromia and titania sols obtained were mixed in the appropriate molar proportions in order to get four compositions: $Cr_{1.95}Ti_{0.05}O_3$, $Cr_{1.9}Ti_{0.1}O_3$, $Cr_{1.8}Ti_{0.2}O_3$, and $Cr_{1.6}Ti_{0.4}O_3$. In order to obtain the nominal composition of $Cr_{1.95}Ti_{0.05}O_3$, 115 ml of the chromia sol (0.1 mol) was mixed with 10.2 ml of the titania sol (2.55×10^{-3} mol).

The resulting mixed sols were dispersed in 350 ml of organic solvent/surfactant solution and stirred with a mechanical stirrer to produce sol droplets. The organic phase chosen was hexane and the emulsifier a non-ionic surfactant (sorbitan monooleate). For all the synthesis, the volume ratio of hexane/sol was kept constant at 3, and the concentration of surfactant was fixed close to 1.5 vol% in hexane, corresponding to the lowest surface tension.[24] The size of the sol spheres was controlled by the stirring. Two different mechanical stirrers with stirring rates varying from 100 to 2000 rpm (KIKA Labortechnik, RW 20.n) and from 8000 to 20500 rpm (KIKA Labortechnik, T25) were used in this study. The different experimental conditions used for the formation of an emulsion are summarised in Table 1. The sol droplets were then gelled by passage of ammonia gas (BOC special gases). The resulting gelled particles were dried at 100 °C overnight in air and then fired at 350 °C with a ramp of temperature of 2 °C min^{-1} before being fired at 1000 °C for 6 hours.

Gas sensing measurements

The CTO powders of composition $Cr_{1.95}Ti_{0.05}O_3$ prepared at the three different stirring rates were each mixed with a commercial carrier (ESL 400) and the inks produced were passed through a triple roll mill to ensure homogeneous dispersion of powder in the vehicle. The inks were screen-printed onto alumina tiles over a double gap gold electrode pattern. The devices were then fired at 800 °C for 2 h, obtained by a temperature ramp of 15 °C min^{-1} to slowly burn off the carrier. Contacts to the devices were formed by spot welding 100 μm diameter platinum wire to the pads. The devices had a platinum heater track, printed on the reverse side of the alumina tile. The sensor was kept at constant resistance and hence at constant temperature by incorporating it into a Wheatstone bridge. Electrical experiments were performed on a locally constructed test rig.[25] Gases were diluted from cylinders of synthetic air (79% N_2, 21% O_2; BOC) containing ethanol (100 ppm). The devices were run at 400 °C in all experiments.

Characterisation

X-Ray powder diffraction patterns of the different samples annealed at 1000 °C were recorded in the region $2\theta=10$–$80°$ with a scanning speed of 0.12° min^{-1} on a Siemens D5000 diffractometer in transmission mode using germanium monochromated Cu $K_{\alpha1}$ ($\lambda=1.5046$ Å) radiation. The average crystallite size of the powders was calculated from the broadening of the (1,0,4) and (1,1,1) diffraction peaks using the Scherrer equation.[9]

Morphological and elemental analyses of the samples were carried out with a Hitachi S570 scanning electron microscope operating at 20 keV and equipped with an energy dispersive X-ray analyser. Samples were coated with either sputtered gold or carbon to reduce charging effects. Both wide area and point EDAX analyses of the powders were performed using cobalt as a reference standard.

XPS measurements were performed on a VG ESCALAB 220i XL instrument using focused (100 μm spot size) monochromatic Al K_α radiation at a pass energy of 20 keV. The binding energies were referenced to the hydrocarbon C 1s peak at 284.8 eV.

Quantification was performed using a Shirley background and sensitivity factors from Wagner *et al.*[26]

Results and discussion

X-Ray powder diffraction patterns of calcined powders of $Cr_{2-x}Ti_xO_{3+y}$ ($x=0.05$, 0.1, 0.2, 0.4), Fig. 1 and 2, indicated a single-phase material when $Ti\leqslant0.2$. Calcination at 1000 °C produced the crystalline eskolaite structure of Cr_2O_3, indicating the formation of a solid solution of TiO_2 in Cr_2O_3. For the highest titanium concentration under study ($Ti=0.4$) an additional low intensity peak at $2\theta=54.8°$ as indicated by * in Fig. 2 was found. According to Somiya *et al.*, the second phase for the relatively high concentration of Ti can be attributed to the presence of $CrTiO_3$ in the sample.[27]

The limit of solubility observed in this study is reached for a higher titanium concentration (10 mol%: $Cr_{1.8}Ti_{0.2}O_3$) for powders prepared by the sol–emulsion–gel route than for those prepared by conventional mixing and calcining,[6] indicating a better mixing of the two phases. The mixing of the Cr_2O_3 and TiO_2 sol at the nanometer scale from the sol–gel route provides a more uniform Ti distribution than the solid state chemical reaction.

No radical change was observed in the crystallite sizes (Table 2) between different samples. A slight decrease in the crystallite size was observed for the powder prepared with low stirring rates (1000 rpm) of nominal composition $Cr_{1.6}Ti_{0.4}O_{3+y}$ (33 nm), whereas the crystallite size (around 40 nm) of the powders obtained at high stirring rates remains constant with increasing titanium content.

Selected SEM images of the calcined samples are shown in Fig. 3 to 5. The micrographs show fairly uniform sized spherical particles. The size of the spherical particles varied with the stirring conditions: the slower the stirring, the larger the particles formed. For example, the average particle size of the powders prepared with a stirrer speed of 1000 rpm was approximately 10 μm (Fig. 3), compared to 2 μm for the samples obtained with a stirring rate of 8000 rpm (Fig. 4) and 0.7 μm for the samples prepared at 20500 rpm (Fig. 5). These microspheres were made up of smaller particles of diameter in

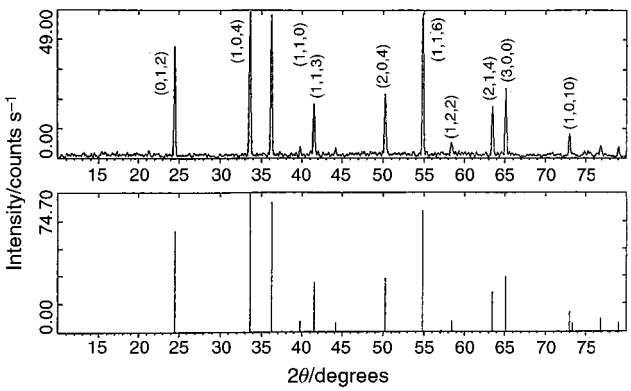

Fig. 1 X-Ray diffraction pattern of the powder fired at 1000 °C of nominal composition $Cr_{1.95}Ti_{0.05}O_3$ obtained from the sol–emulsion–gel route with a stirring rate of 2000 rpm compared to the JCPDS reference pattern.

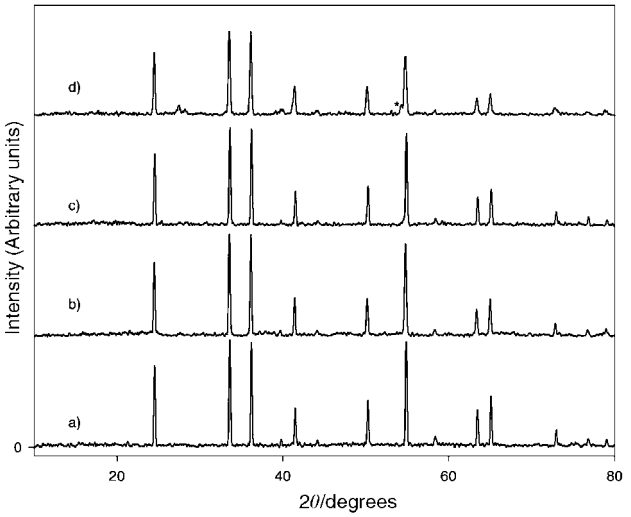

Fig. 2 X-Ray diffraction patterns of the compounds from the sol–emulsion–gel route with a stirring rate of 2000 rpm fired at 1000 °C with nominal compositions: a) $Cr_{1.95}Ti_{0.05}O_3$, b) $Cr_{1.9}Ti_{0.1}O_3$, c) $Cr_{1.8}Ti_{0.2}O_3$ and d) $Cr_{1.6}Ti_{0.4}O_3$.

the range of 0.1 to 0.2 μm, resulting in the microspheres being themselves porous. Larger pores were observed between the spherical grains and the size of these pores decreased with the particle size. Some of the particles were broken and not completely spherical. This is the first reported preparation of submicrometer spherical particles using the sol–emulsion–gel technique. The previous studies in the literature have described the formation of larger particles (20 to 100 μm) of Cr_2O_3,[7] $ZrTiO_4$[8] and Y_2O_3–ZrO_2.[14]

Wide area (spot size 100 μm) EDAX analysis of the different samples confirmed a close correlation between the achieved average bulk compositions and the nominal compositions (Table 3). Spot analysis (spot size of 2 μm) was also in close agreement with expected values indicating a good compositional homogeneity. No impurity was detected by EDAX analysis.

XPS spectra of the Cr 2p core levels of the $Cr_{2-x}Ti_xO_3$ samples obtained using a stirring rate of 1000 rpm are shown in Fig. 6. The binding energy positions of the Cr $2p_{3/2}$, Ti $2p_{3/2}$ and O 1s levels of the CTO powders are given in Table 4. No significant variation in the positions of the Cr $2p_{3/2}$, Ti $2p_{3/2}$ levels is observed between the different compositions and fabrication procedures. The binding energy positions of the Cr $2p_{3/2}$, Ti $2p_{3/2}$ and O 1s levels are in good agreement with literatures values.[1]

The Cr $2p_{3/2}$ peaks of all the CTO powders showed a double peak at around 577 eV attributed to Cr^{3+} and a minor component at around 580 eV attributed to Cr^{6+}.[28] A large surface segregation of Ti is found: Fig. 7 shows the variation of the surface Ti atomic concentration determined by XPS *versus* the Ti atomic concentration obtained by EDAX. XPS is a surface sensitive technique, interrogating at most the top 10

Table 2 Crystallite size of the CTO powders prepared from different procedures for different titanium concentrations

Procedure	Nominal composition	Crystallite size/nm
A	$Cr_{1.95}Ti_{0.05}O_3$	40
	$Cr_{1.9}Ti_{0.1}O_3$	37
	$Cr_{1.8}Ti_{0.2}O_3$	39
	$Cr_{1.6}Ti_{0.4}O_3$	33
B	$Cr_{1.95}Ti_{0.05}O_3$	36
	$Cr_{1.9}Ti_{0.1}O_3$	38
	$Cr_{1.6}Ti_{0.4}O_3$	39
C	$Cr_{1.95}Ti_{0.05}O_3$	36
	$Cr_{1.9}Ti_{0.1}O_3$	40

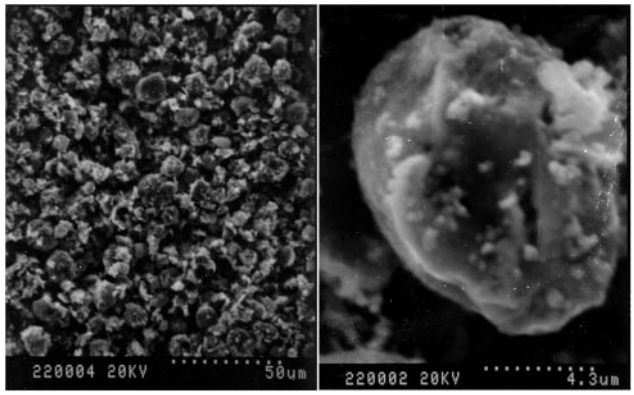

Fig. 3 Scanning electron micrographs of the CTO powder obtained from the sol–emulsion–gel route with a stirring rate of 2000 rpm, calcined at 1000 °C, at two different magnifications.

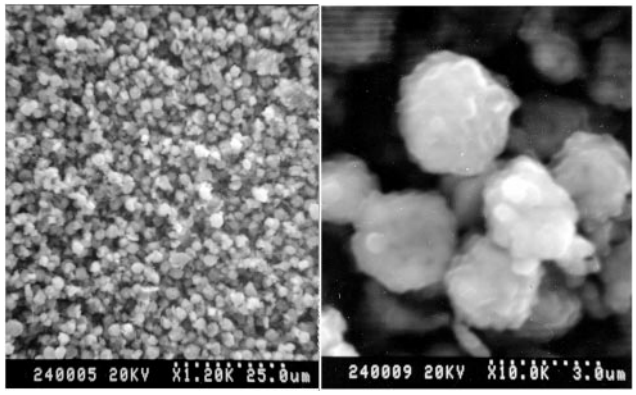

Fig. 4 Scanning electron micrographs of the CTO powder obtained from the sol–emulsion–gel route with a stirring rate of 8000 rpm, calcined at 1000 °C, at two different magnifications.

atom layers only whilst the EDAX excitation volume at the accelerating voltage used analysed the composition from 1–3 μm beneath the surface, hence giving a bulk analysis. Fig. 7 shows that the variation of surface segregation with bulk titanium composition depended to some extent on the preparation procedure. The surface Ti concentration appears to increase linearly with Ti doping for the powders prepared at a stirring rate of 8000 rpm (note, however, only three data points), whereas the shape of the curve showing the surface Ti concentration with the bulk composition from the powders obtained at a stirring rate of 1000 rpm is convex.

The $Cr_{1.95}Ti_{0.05}O_3$ microspheres were screen-printed onto pre-patterned alumina substrates that contained double gold electrode gaps. Resistance measurements were taken between

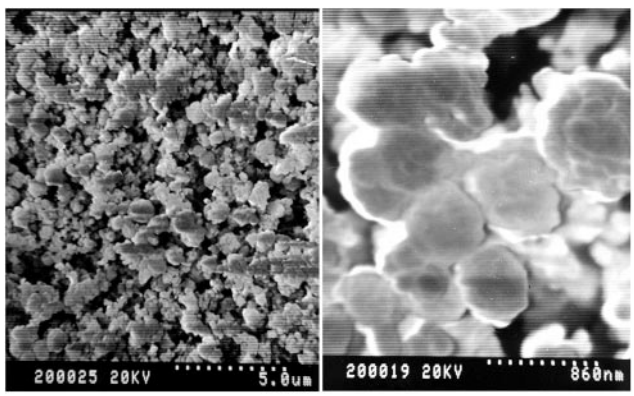

Fig. 5 Scanning electron micrographs of the CTO powder obtained from the sol–emulsion–gel route with a stirring rate of 20500 rpm, calcined at 1000 °C, at two different magnifications.

Table 3 EDX analysis of Cr and Ti

	Nominal composition		Broad beam		Spot beam	
Procedure	Cr (at%)	Ti (at%)	Cr (at%)	Ti (at%)	Cr (at%)	Ti (at%)
A	97.5	2.5	97.65	2.405	97.8	2.2
	95	5	94.8	5.2	95.8	4.2
	90	10	89.98	10.02	90.02	9.92
	80	20	78.71	21.29	78.2	21.8
B	97.5	2.5	97.2	2.8	97.8	2.2
	95	5	94.71	5.29	94.48	5.52
	80	20	78.13	21.87	77.39	22.61
C	97.5	2.5	97.62	2.38	97.55	2.45
	95	5	95.06	4.94	95.64	4.36

Table 4 XPS binding energies for $Cr_{2-x}Ti_xO_{3+y}$ from the different procedures

Procedure	Nominal composition	Cr $2p_{3/2}$	Ti $2p_{3/2}$	O 1s
A	$Cr_{1.95}Ti_{0.05}O_3$	576.7	458	530.1
	$Cr_{1.9}Ti_{0.1}O_3$	577.2	458.4	530.5
	$Cr_{1.8}Ti_{0.2}O_3$	577.1	458.3	530.4
	$Cr_{1.6}Ti_{0.4}O_3$	577.3	458.3	530.4
B	$Cr_{1.95}Ti_{0.05}O_3$	577	458.2	530.6
	$Cr_{1.9}Ti_{0.1}O_3$	577	458.3	530.5
	$Cr_{1.6}Ti_{0.4}O_3$	577	458.6	530.4
C	$Cr_{1.95}Ti_{0.05}O_3$			
	$Cr_{1.9}Ti_{0.1}O_3$			

the large and common electrodes, with a 150 μm gap (R_L) and between the small and common electrodes, with a 20 μm gap (R_s). The bound materials were fired and then used to determine the gas response to ethanol vapour in dry and humid air, at 400 °C, Fig. 8. Three separate sensor materials were tested, all of composition $Cr_{1.95}Ti_{0.05}O_3$; one sensor for each of the different stirring rates 2000, 8000 and 20500 rpm (labelled A, B and C respectively in Fig. 8). All of the materials functioned extremely well as ethanol sensors, giving significant and reproducible changes of resistance with ethanol concentration in both dry and humid air.

Three main microstructure effects can be observed from these measurements. Firstly, the sensitivity (R/R_o) to ethanol decreases with the particle size. This decrease is much more effective between sensors B (2 μm particle diameter) and C

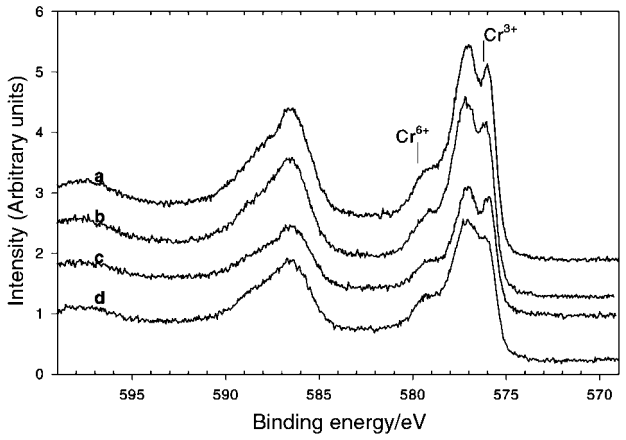

Fig. 6 XPS spectra of the Cr 2p core level of the $Cr_{2-x}Ti_xO_3$ samples obtained from the sol–emulsion–gel route with a stirring rate of 2000 rpm: a) $Cr_{1.95}Ti_{0.05}O_3$, b) $Cr_{1.9}Ti_{0.1}O_3$, c) $Cr_{1.8}Ti_{0.2}O_3$ and d) $Cr_{1.6}Ti_{0.4}O_3$.

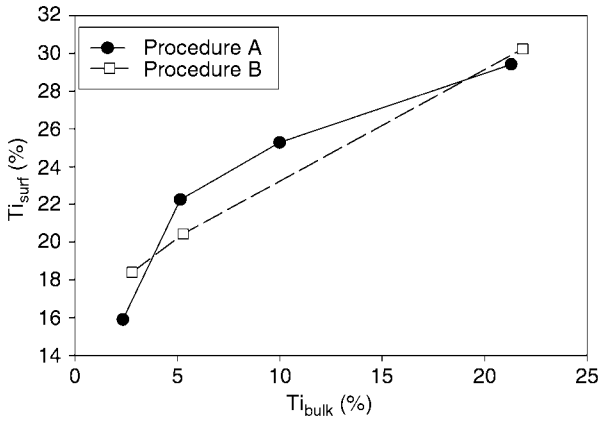

Fig. 7 Variation of the Ti concentration at the surface as a function of the Ti concentration in the bulk.

(0.7 μm particle size) than between sensors A (10 μm particle size) and B. Secondly, a finer microstructure provides a decrease of the response time as shown in Fig. 8: the sensor prepared from C with the smaller particle sizes comes back to the baseline more rapidly than the other sensors. The third effect of the microstructure is that the ethanol response to the small and common electrodes compared to the large and common electrodes is reduced as the microstructure become finer. For example, the ratio of the large gap electrode response ($(R/R_o)_L$) to the small one ($(R/R_o)_s$) increases from 1.20 for sensor A to 1.36 for sensor B and to 1.50 for sensor C.

No significant influence of humidity was observed on the response of any of the sensors to ethanol; however, the response of the sensors was increased by 10 to 20% in the presence of humidity.

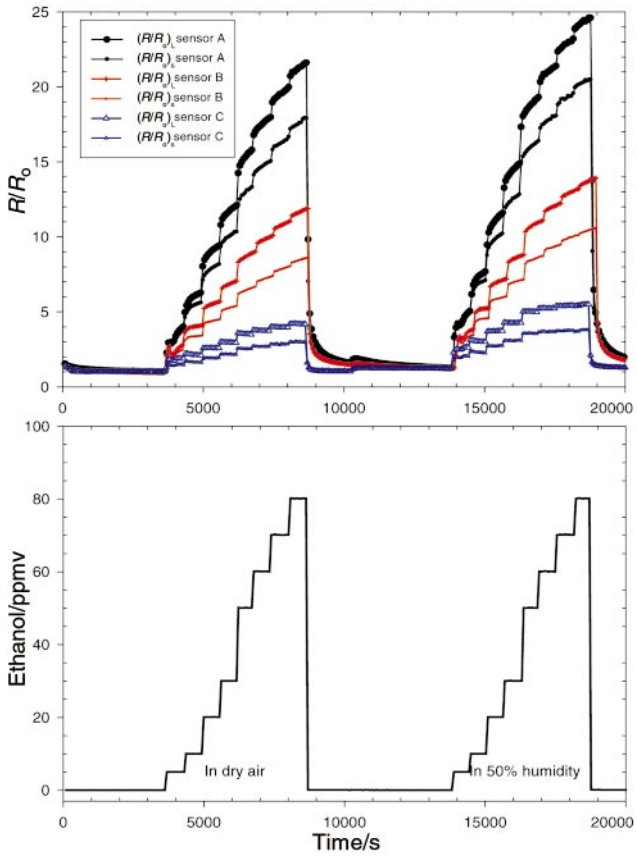

Fig. 8 Resistance ratio, R/R_o (where R_o represents the resistance in dry air), of the sensors A, B and C responding to different concentrations of ethanol in dry air and in air of 50% humidity.

Conclusion

$Cr_{2-x}Ti_xO_{3+y}$ microspheres of composition varying from $x=0.05$, 0.1, 0.2, 0.4 were prepared for the first time by the sol–emulsion–gel method. Three different-scale particles of fairly uniform spherical particles and of a good compositional homogeneity were obtained by varying the stirring rate of the emulsion. Submicrometer spherical particles (0.7 μm) of CTO were produced at high stirring rates. The characterisation by XRD of the powders calcined at 1000 °C has shown the formation of a single-phase material for $Cr_{1.95}Ti_{0.05}O_3$, $Cr_{1.9}Ti_{0.1}O_3$ and $Cr_{1.8}Ti_{0.2}O_3$ and the appearance of a second phase for $Cr_{1.6}Ti_{0.4}O_3$, independent of the preparative procedure. The EDAX and XPS measurements have confirmed the absence of impurities in the prepared powders and have revealed a large surface segregation of the Ti atoms. These spherical particles of CTO showed good stability: their composition and microstructures remained unaffected by firing up to 1000 °C. The CTO materials when bound as sensors show excellent responses to ethanol concentration in air. The magnitude of the ethanol response was directly proportional to the microstructure of the material with the largest particles giving the greatest changes in resistivity. Further work on the gas sensing properties of these materials is in progress.

Acknowledgements

This work was supported by the European Commission. We also thank Bernie Hutton for carrying out the XPS work.

References

1 G. S. Henshaw, D. H. Dawson and D. E. Williams, *J. Mater. Chem*, 1995, **5**(11), 1791.
2 P. T. Moseley and D. E. Williams, *Sens. Actuators B*, 1990, **1**, 113.
3 D. H. Dawson, G. S. Henshaw and D. E. Williams, *Sens. Actuators B*, 1995, **26**(1–3), 76.
4 D. E. Williams, *Sens. Actuators B*, 1999, **57**(1–3), 1.
5 K. F. E. Pratt and D. E. Williams, *Sens. Actuators B*, 1997, **45**, 147.
6 V. Jayaraman, K. I. Gnanasekar, E. Prabhu, T. Gnanasekaran and G. Periaswami, *Sens. Actuators B*, 1999, **55**, 175.
7 M. Chatterjee, B. Siladitya and D. Ganguli, *Mater. Lett.*, 1995, **25**, 261.
8 A. K. Bhattacharya, K. K. Mallick, A. Hartridge and J. L. Woodhead, *J. Mater. Sci.*, 1996, **31**, 267.
9 A. K. Bhattacharya, A. Hartridge, K. K. Mallick and J. L. Woodhead, *J. Mater. Sci.*, 1994, **29**, 6076.
10 F. G. Sherif and L. J. Shyu, *J. Am. Ceram. Soc*, 1991, **74**(2), 375.
11 K. T. Scott and J. L. Woodhead, *Thin Solid Films*, 1982, **95**, 219.
12 D. Segal, *J. Mater. Chem.*, 1997, **7**(8), 1297.
13 J. L. Woodhead, *J. Mater. Educ.*, 1984, **6**, 887.
14 M. Chatterjee, J. Ray, A. Chatterjee, D. Ganguli, S. V. Joshi and M. P. Srivastava, *J. Mater. Sci.*, 1993, **28**, 2803.
15 A. K. Bhattacharya and A. Hartridge, *J. Mater. Sci. Lett.*, 1996, **15**, 1846.
16 R. Sella, A. Serra, P. Siciliano, L. Vasanelli, G. De, A. Licciulli and A. Quirini, *Sens. Actuators B*, 1997, **44**, 462.
17 S. G. Ansari, P. Boroojerdian, S. R. Sainkar, R. N. Karekar, R. C. Aiyer and S. K. Kulkarni, *Thin Solid Films*, 1997, **295**, 271.
18 J. P. Chatelon, C. Terrier, E. Bernstein, R. Berjoan and J. A. Roger, *Thin Solid Films*, 1994, **247**, 162.
19 A. Wilson, J. D. Wright, J. Murphy, M. A. M. Stroud and S. C. Thorpe, *Sens. Actuators B*, 1994, **18–19**, 506.
20 S. S. Park and J. D. Mackenzie, *Thin Solid Films*, 1995, **258**, 268.
21 J. R. Bartlett, D. Gazeau, T. H. Zemb and J. L. Woolfrey, *J. Sol–Gel Sci. Technol.*, 1998, **13**, 113.
22 M. A. Anderson, M. J. Gieselmann and Q. Xu, *J. Membr. Sci.*, 1988, **39**, 243.
23 D. Vorkapic and T. Matsoukas, *J. Am. Ceram. Soc.*, 1998, **81**(11), 2815.
24 M. Chatterjee, G. S. Nasker, B. Siladitya and D. Ganguli, *J. Mater. Res.*, 2000, **15**(1), 176.
25 G. S. Henshaw, D. H. Dawson and D. E. Williams, *J. Mater. Chem.*, 1995, **5**, 1791.
26 C. D. Wagner, L. E. Davis, M. V. Zeller, J. A. Taylor, R. H. Raymond and L. H. Gale, *Surf. Interface Anal.*, 1981, **3**, 211.
27 S. Somiya, H. Hirano and S. Kamiya, *J. Solid State Chem.*, 1978, **25**, 273.
28 C. D. Wagner, in *Practical Surface Analysis, Auger and X-ray Photoelectron Spectroscopy*, ed. D. Briggs and M. P. Seah, Wiley, Chichester, 2nd edn.,1990, vol. 1, p. 595.